Novel Decentralized Pole Placement Design of Power System Stabilizers Using Hybrid Differential Evolution

Yung-Sung Chuang, Shu-Chen Wang, and Chi-Jui Wu

Abstract**—**This paper is used to investigate a novel decentralized pole placement design of lead-lag power system stabilizers using hybrid differential evolution (HDE). Since only local speed deviations are used as the feedback signals, the decentralized stabilizers could be easily implemented. It wants to place the electromechanical modes within a designated region to have enough damping. Participation factors are used to select the site and number of stabilizers. If all electromechanical modes have been moved to the specified region at the convergent step, the objective function will reach a minimal value. The objective function is chosen to ensure the real parts and damping ratios of electromechanical modes. A test power system is used to reveal the goodness of this method. Several operating points can be considered simultaneously in the determination of stabilizer parameters to let the stabilizers work well under a wider range of operating conditions. The computation time and convergence characteristic of this approach are better, compared to the differential evolution and genetic algorithm. The coherency measures are also proposed to evaluate the relative behaviors between any pair of generators of the system with and without stabilizers.

Keywords**—**Power system stabilizer, electromechanical mode, pole placement, hybrid differential evolution, power system dynamics, lead-lag power system stabilizers.

I. Introduction

The dynamic stability characteristics of a power system are affected by the location of electromechanical modes. It is sufficient that all electromechanical modes are placed in a suitable region in the complex variable plane to ensure damping effects on low frequency oscillations. Power system stabilizers (PSSs) have been widely used to increase the damping forces of electromechanical modes. Recently, design technology has been focused on how to tune PSSs in order to obtain suitable dynamic stability characteristics. Those methods include the optimization method using eigenvalue analysis [1], genetic design using simulated annealing optimization algorithms [2], probabilistic approach [3], Tabu search algorithm [4], particle-swarm-optimization technique [5], and genetic algorithm [6].

The hybrid differential evolution (HDE) is one of the best evolutionary algorithms for solving non-linear optimization problems [7]-[8]. A lot of works have been recoded about the applications of HDE. It has been applied to the optimal control problem of a bio-process system [9]. Estimating the kinetic model parameters using HDE was presented in other literature [10]. It was also employed in plant scheduling and planning to solve the decision-making problems of the manufacturing industry [11]. The improved HDE method has been used to reduce power loss and enhance the voltage profile [12]. It may determine the optimal capacitor location of a radial distribution feeder [13].

The HDE is applied in this paper to tune the lead-lag type PSSs. Participation factors are used to determine the sites and number of PSSs [14]-[15]. The local generator speed feedback signals are applied to have decentralized control schemes [16]-[17]. It is to move all electromechanical modes to a designated region in the complex variable plane. The objective function is selected to ensure the real parts and damping ratios of electromechanical modes. At the convergent step, if all electromechanical modes have been moved to the designated region, the objective function will converge to zero, which is the minimal value. From the simulation results of a multi-machine power system, the PSSs can let the generators have enough damping forces when there are line-tripping disturbances. The computation time and design results are better, compared with that using the differential evolution (DE) and genetic algorithm (GA). From the results of coherency measures, the levels of similarity between any pair of generators have been kept.

II. Hybrid Differential Evolution

A nonlinear optimization problem can be expressed as

$$\text{Minimize } M(\mathbf{X}) \tag{1}$$

Subject to

$$g_k(\mathbf{X}) \le 0 \qquad k = 1, \ldots, n_g \tag{2}$$

Manuscript received April 10, 2007; Revised received December 23, 2007.

Yung-Sung Chuang is with the Department of Electrical Engineering, Ming Hsin University of Science and Technology, Hsin Feng, Hsin Chu, 304, Taiwan. (e-mail: d8507001@mouse.ee.ntust.edu.tw).

Shu-Chen Wang is with the Department of Computer and Communication Engineering, Taipei College of Maritime Technology, 212, Sec. 9, Yan-Pin N. Rd., Taipei 111, Taiwan (corresponding author to provide phone: 886-2-27376676; fax: 886-2-27376699; e-mail: scwang@mail.tcmt.edu.tw).

Chi-Jui Wu is with the Department of Electrical Engineering, National Taiwan University of Science and Technology, 43, Keelung Rd., Sec. 4, Taipei 106, Taiwan. (e-mail: cjwu@mail.ntust.edu.tw).

$$h_k(\mathbf{X}) = 0 \qquad k = 1, \dots, n_h \tag{3}$$

where $M(\mathbf{X})$:objective function of variable vector $\mathbf{X}$,

$$\mathbf{X} = \left[\mathbf{X}_1, \mathbf{X}_2, .., \mathbf{X}_j, .., \mathbf{X}_D \right]^{\mathrm{T}}$$

$g_k(\mathbf{X})$: inequality constraints.

$h_k(\mathbf{X})$: equality constraints.

Differential evolution is a parallel direct search method for minimizing nonlinear and non-differential objective functions. The fitness of an offspring is determined by one-to-one competition with the corresponding parent. The solution procedures are given as follows.

Step 1. Initialization: Several initial populations $\mathbf{X}_i^0, i = 1, 2, \dots, N_P$ are randomly selected. They should cover the entire search space uniformly. The elements of each individual $\mathbf{X}_i^0$ are given by

$$X_{ji}^0 = X_j^{min} + \rho_i (X_j^{max} - X_j^{min})$$
$$j = 1, 2, \dots, D \;, i = 1, 2, \dots, N_p \tag{4}$$

where $\rho_i \in [0,1]$ is a random number, and N_P is the population size. X_j^{min} and X_j^{max} are the lower and upper bounds of the variable X_j, respectively.

Step 2. Mutation operation: At generation G, each mutant vector is generated based on the corresponding present individual $\mathbf{X}_i^G$ by

$$\mathbf{U}_i^{G+1} = \mathbf{X}_i^G + F(\mathbf{X}_{r1}^G - \mathbf{X}_{r2}^G), \;\; i = 1, 2, \dots, N_p \tag{5}$$

where $i \neq r1, i \neq r2,$ and $r1, r2 \in \{1, 2, \dots N_P\}$. $F \in [0,1]$ is a scalar factor. $\underline{X}_{r1}^G$ and $\underline{X}_{r2}^G$ are two randomly selected individuals.

Step 3. Crossover operation: To extend the diversity of individuals in the next generation, the perturbed individual $\mathbf{U}_i^{G+1} = \left[U_{1i}^{G+1}, U_{2i}^{G+1}, .., U_{ji}^{G+1}, .., U_{Di}^{G+1} \right]^{\mathrm{T}}$ and the present individual $\mathbf{X}_i^G = \left[X_{1i}^G, X_{2i}^G, \dots, X_{ji}^G, .., X_{Di}^G \right]^{\mathrm{T}}$ are mixed to yield the trial vector

$$\hat{\mathbf{U}}_i^{G+1} = \left[\hat{U}_{1i}^{G+1}, \hat{U}_{2i}^{G+1}, .., \hat{U}_{ji}^{G+1}, .., \hat{U}_{Di}^{G+1} \right]^{\mathrm{T}} \tag{6}$$

where

$$\hat{U}_{ji}^{G+1} = \begin{cases} X_{ji}^G, if \quad a \;\; random \;\; number > C_R \\ U_{ji}^{G+1}, otherwise \end{cases}$$
$$j = 1, 2, \dots, D \qquad , \qquad i = 1, 2, \dots, N_P$$

(7)

where D is also the number of genes. $C_R \in [0,1]$ is the crossover factor and must be set by the user.

Step 4. Evaluation and selection: The parent is replaced by its offspring in the next generation if the fitness of the latter is better. Contrarily, the parent is retained. The first step is one-to-one competition. The next step chooses the best individual, $\mathbf{X}_b^{G+1}$ in the population. That is

$$\mathbf{X}_i^{G+1} = arg\text{-}min \{ M(\mathbf{X}_i^G), M(\hat{\mathbf{U}}_i^{G+1}) \}$$
$$i = 1, 2, \dots, N_P \tag{8}$$

$$\mathbf{X}_b^{G+1} = arg\text{-}min \{ M(\mathbf{X}_i^{G+1}) \}, i = 1, 2, \dots, N_P \tag{9}$$

where *arg-min* means the argument of the minimum.
The above steps are repeated until the maximum iteration number or the desired fitness is obtained. In general, a faster descent usually leads to a local minimum or a premature convergence. Conversely, diversity guarantees a high probability of obtaining the global optimum. The trade-off can be obtained by slightly lowering the scaling factor F and by increasing the population size N_P . However, more computation time is required. The migrant and accelerated operations in HDE are used to overcome the local minimum solution and time consumption. The migrant and accelerating operations are inserted in the differential evolution.

Step 5. Migrant operation if necessary: For increasing search space exploration, a migration operation is introduced to regenerate a diverse population of individuals. The migrant individuals are selected on a "best individual" basis $\mathbf{X}_b^{G+1}$. The j[th] gene of $\mathbf{X}_i$ is regenerated by

$$X_{ji}^{G+1} = \begin{cases} X_{jb}^{G+1} + \rho_1 (X_j^{\min} - X_{jb}^{G+1}), & if \; a \;\; ramdom \;\; number \;\; \rho_2 < \dfrac{X_{jb}^{G+1} - X_j^{\min}}{X_j^{\max} - X_j^{\min}} \\ X_{jb}^{G+1} + \rho_1 (X_j^{\max} - X_{jb}^{G+1}), & otherwise \end{cases} \tag{10}$$

where ρ_1 and ρ_2 are randomly generated numbers uniformly distributed in [0, 1]. The migrant population will not only become a set of newly promising solutions, but also avoid the local minimum trap.

The migrant operation is performed only if a measure fails to match the desired population diversity tolerance. The measure in this study is defined as

$$u = \frac{\left[\sum\limits_{\substack{i=1 \\ i \neq b}}^{N_P} \sum\limits_{j=1}^{D} \eta_{ji} \right]}{D(N_P - 1)} < \varepsilon_1 \tag{11}$$

where

$$\eta_{ji} = \begin{cases} 1, & if \quad \left| \dfrac{X_{ji}^{G+1} - X_{jb}^{G+1}}{X_{jb}^{G+1}} \right| > \varepsilon_2 \\ 0, & otherwise \end{cases} \tag{12}$$

parameters $\varepsilon_1 \in [0,1]$ and $\varepsilon_2 \in [0,1]$ express the desired tolerance of the population diversity and the gene diversity with regard to the best individual, respectively. Here η_{ji} is defined as an index of the gene diversity. A zero η_{ji} means that the j^th^ gene of the i^th^ individual is close to the j^th^ gene of the best individual. If the degree of population diversity u is smaller than ε_1, the HDE performs migration to generate a new population to escape the local point. Otherwise, HDE breaks off the migration, which maintains an ordinary search direction.

Step 6. Accelerated operation if necessary: When the fitness in the present generation is no longer improved using the mutation and crossover operations, a descent method is then applied to push the present best individual toward a better point. Thus, the acceleration operation can be expressed as

$$\hat{\mathbf{X}}_b^{G+1} = \begin{cases} \mathbf{X}_b^{G+1}, & if\ a\ \ objective\ \ function\ \ M(\mathbf{X}_b^{G+1}) < M(\mathbf{X}_b^G) \\ \mathbf{X}_b^{G+1} - \alpha \nabla M(\mathbf{X}_b^{G+1}), & otherwise \end{cases} \tag{13}$$

The gradient of the objective functions, $\nabla M(\mathbf{X}_b^{G+1})$, can be approximately calculated with a finite difference. The step size $\alpha \in (0,1]$ is determined according to the decent property. Firstly, α is set to unity. The objective function $M(\hat{\mathbf{X}}_b^{G+1})$ is then compared with $M(\mathbf{X}_b^{G+1})$. If the decent property is achieved, $\hat{\mathbf{X}}_b^{G+1}$ becomes a candidate in the next generation, and is added into this population to replace the worst individual. On the other hand, if the decent requirement fails, the step size is reduced, for example, 0.5 or 0.7. The decent search method is repeated to find the optimal $\hat{\mathbf{X}}_b^{G+1}$, called $\mathbf{X}_b^N$, at the (G+1)^th^ generation. This result shows the objective function $M(\mathbf{X}_b^N)$ should be at least equal or smaller than $M(\mathbf{X}_b^{G+1})$.

III. Decentralized Pole Placement Design

A. Power system description

Determining the parameters of PSSs for an N-generator power system should consider various loading conditions. The equations of generator i in the linearized two-axis model are expressed by

$$\dot{\mathbf{x}}_i(\mathbf{t}) = \mathbf{A}_{ii}\mathbf{x}_i(\mathbf{t}) + \sum_{j=1, j \neq i}^{N} \mathbf{A}_{ij}\mathbf{x}_j(\mathbf{t}) + \mathbf{B}_{ii}\mathbf{u}_i(\mathbf{t}) \qquad i = 1,2,...,N \tag{14}$$

where $\mathbf{x}_i(t) = [\Delta E'_{di} \quad \Delta E'_{qi} \quad \Delta\omega_i \quad \Delta\delta_i \quad \Delta E_{FDi} \quad \Delta V_{Si}\quad]^T$ is the state vector, $\Delta E'_{di}$ and $\Delta E'_{qi}$ are the d-axis and q-axis transient voltages, respectively, $\Delta\omega_i$ and $\Delta\delta_i$ are the generator speed and angle, respectively, ΔE_{FDi} is the field voltage, and ΔV_{Si} is the output signal of stabilizing transformer. The simplified static excitation system is given in Fig. 1.

B. Lead-lag PSS

The lead-lag phase compensation PSS is considered as shown in Fig. 2. The local generator speed deviations are used as the feedback signals. The transfer function is

$$u(s) = K_S \frac{sT_5}{1+sT_5}\left(\frac{(1+sT_1)(1+sT_3)}{(1+sT_2)(1+sT_4)}\right)\Delta\omega(s) \tag{15}$$

If the washout time constant, T_5, is given, the remaining parameters, K_S, T_1, T_2, T_3, and T_4, are to be determined.

C. Objective function

The objective function is selected so that all electromechanical modes can be moved to the specified region as shown in Fig. 3. It is required that $\sigma_{i,j} \le \sigma_0$ and $\zeta_{i,j} \ge \zeta_0$, where $\sigma_{i,j}$ and $\zeta_{i,j}$ are the real part and damping ratio of the ith electromechanical mode under the jth operating condition. Then the objective function for an N-generator system is given by

$$M = \sum_{j=1}^{np}\sum_{i=1}^{N}\left(\sigma_0 - \sigma_{i,j}\right)^2 + \sum_{j=1}^{np}\sum_{i=1}^{N}\left(\zeta_0 - \zeta_{i,j}\right)^2 \tag{16}$$

$$for \quad \sigma_{i,j} \ge \sigma_0 \quad and \quad \zeta_{i,j} \le \zeta_0$$

where np is the number of operating points considered simultaneously in the design procedures. The system stability condition is determined by the damping constant, σ_0, and damping ratio, ζ_0. In the design procedures using the HDE, the population size, N_P, is selected to be 5, the scalar factor, F, to be 0.01, and the crossover factor, C_R, to be 0.5.

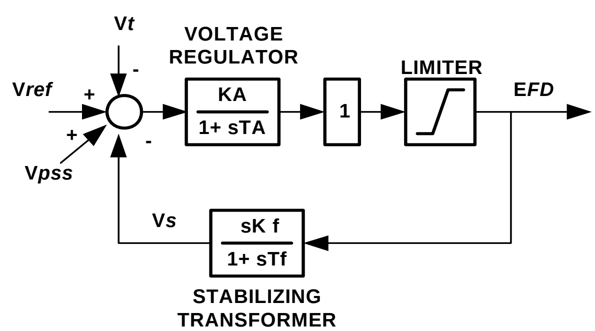

Fig. 1. Block diagram of static excitation system

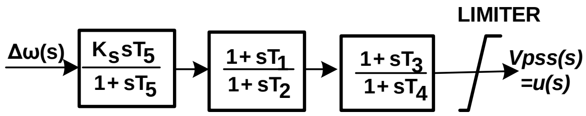

Fig. 2. Block diagram of lead-lag phase compensation power system stabilizer

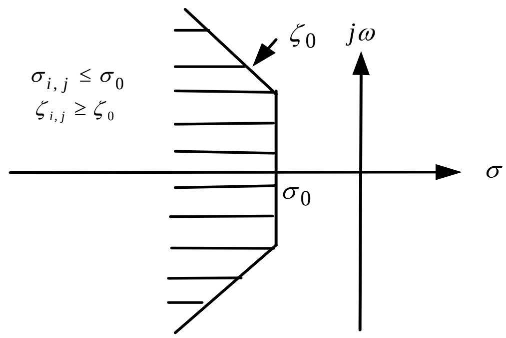

Fig. 3. A region where $\sigma_{i,j} \le \sigma_0$ and $\zeta_{i,j} \ge \zeta_0$

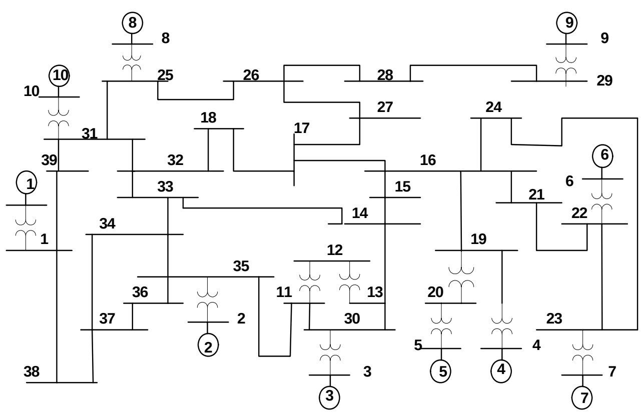

Fig. 4. The test power system

IV. EXAMPLE: A MULTI-MACHINE SYSTEM

Consider the test power system as shown in Fig. 4 where bus 1 is assumed to be an infinite bus. Generators 2-10 (G2-G10) are equipped with static exciters. The system data are given in [18]. The electromechanical modes of the system are shown in the first column of Table 1. Some damping characteristics of electromechanical modes are poor, especially that of $-0.06 \pm j6.68$ and $-0.10 \pm j3.16$.

The participation factors from summation of $\Delta\delta$ and $\Delta\omega$ of each generator associated with the electromechanical modes are also given in Table 1. G10 is chosen to install a PSS to enhance the worst damping mode $-0.06 \pm j6.68$. G9 is suitable to install a PSS and improve the mode $-0.10 \pm j3.16$. The other suitable sites are G2, G4 and G7.

A. Comparison of HDE, DE, and GA

In the designing PSSs of G2, G4, G7, G9, and G10 using DE, GA, and HDE, it is selected that $\sigma_0 = -0.5$ and $\zeta_0 = 0.1$. The convergent results are revealed in Fig. 5. The computation time is evaluated by the CPU time as shown in Table 2. It indicates that HDE is faster than GA. Although DE is the fastest, it converges to a local optimal solution and has a larger convergent objective function. The designed parameters of PSSs are given in rows 2-4 of Table 3. The electromechanical modes of the system with DE_PSS, GA_PSS, and HDE_PSS under operation condition 1 are tabulated in Table 4.

In the time domain simulations, nonlinear differential equations must be used to examine the damping effects of PSSs. The tripping of line 1-38 is used as a larger disturbance. Simulation results are given in Fig. 6 for generators 2, 4, 7, 9, and 10. The system with the HDE_PSS has better responses.

B. Design under different operation conditions

In the design of PSSs using HDE, three operating conditions can be considered simultaneously.

Operating condition 1: Normal load.

Operating condition 2: Remove of line 1-38.

Operating condition 3: Remove of line 21-22, and 25 % load increase at buses 16 and 21, and 25% generation increase at G7.

It is also selected that $\sigma_0 = -0.5$ and $\zeta_0 = 0.1$. Fig. 7 shows the comparison of convergent characteristic. The designed parameters of PSSs considering operation conditions 1-3 simultaneously are given in Table 5. The electromechanical modes designed under operating condition 1 only and operation condition 1-3 simultaneously are shown in the third row and fourth row of Table 6. For the system to have damping forces under a wider operation conditions, the designed PSSs under operation condition 1-3 simultaneously should be better than that under operation condition 1 only.

C. Comparison of different objective function

Two additional objective functions are compared with the M in (16).

(A) The objective function to emphasize the damping constants is

$$M_1 = \sum_{j=1}^{np} \sum_{i=1}^{N} \left(\sigma_0 - \sigma_{i,j}\right)^2, \qquad for \quad \sigma_{i,j} \ge \sigma_0 \tag{17}$$

A shape in which $\sigma_{i,j} \le \sigma_0$ is shown in Fig. 8. The design results want to force electromechanical modes to locate on the left side of the vertical line $\sigma = \sigma_0$.

(B) The objective function to emphasize the damping ratios is

$$M_2 = \sum_{j=1}^{np} \sum_{i=1}^{N} \left(\zeta_0 - \zeta_{i,j}\right)^2, \quad for \quad \zeta_{i,j} \le \zeta_0 \tag{18}$$

This wants to put all electromechanical modes in a sector in which $\zeta_{i,j} \ge \zeta_0$ as shown in Fig. 9 to ensure every electromagnetic mode has a damping ratio no less than the specified ζ_0.

In the designing PSSs of G2, G4, G7, G9, and G10 using HDE considering operation conditions 1-3 simultaneously, it is also selected that $\sigma_0 = -0.5$ and $\zeta_0 = 0.1$. Fig. 10 shows the comparison of convergent characteristics. The designed parameters of PSSs using M_1 and M_2 are given in Table 7. The electromechanical modes are given in the third, fourth, and fifth rows of Table 8, respectively. When the objective function M is used, the system has best dynamic characteristics.

TABLE I
PARTICIPATION FACTORS OF GENERATOR SPEED AND ROTOR ANGLE OF THE SYSTEM WITHOUT PSS

Electromechanical mode (Damping Ratio)	G2	G3	G4	G5	G6	G7	G8	G9	G10
-0.49 ± j 9.48 (0.05)	0	0	-0.16	-0.01	0.73	1.50	0	0	0
-0.40 ± j 9.21 (0.04)	0	0	1.80	0.18	0.11	0.16	0.09	0	0
-0.42 ± j 8.80 (0.05)	0.01	0.01	0.05	0.01	0.05	0	1.80	0.04	0.09
-0.24 ± j 7.99 (0.03)	1.03	0.98	0	0	0	0	0	0	0
-0.26 ± j 7.08 (0.04)	0.30	0.24	0.01	0.24	0.82	0.40	0	0.03	0.01
-0.06 ± j 6.68 (0.01)	0.14	0.17	0	0.06	0.05	0.03	0.02	0.05	1.49
-0.19 ± j 6.03 (0.03)	0.39	0.42	0	0.39	0.02	0.02	0.01	0.61	0.15
-0.20 ± j 5.91 (0.04)	0	0	0.08	0.82	0.02	0.01	0.04	0.92	0.12
-0.10 ± j 3.20 (0.03)	0.14	0.18	0.24	0.36	0.27	0.23	0.09	0.36	0.14

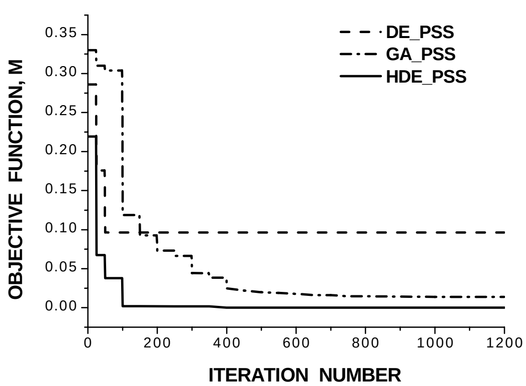

Fig. 5. Convergent characteristics of objective functions, M, using DE, GA, and HDE

D. Coherency analysis

The coherency measures derived from responses in Fig. 6 are proposed to evaluate the relative behaviours between any pair of generators. The results are given in Table 9 and Table 10 for the system without and with the PSSs, respectively. It can be found that the levels of similarity have been kept. For example, the values in Table 9 show that G2 has a higher relation with G3. This situation also can be found in Table 10. Since the coherency behaviours do not be destroyed, the system should have a higher stability condition.

TABLE II
COMPARISON OF DE, GA, AND HDE

DE	Objective Function (pu)	N_P	CPU time (sec)	C_R	F
	0.0963	5	7.7776	0.5	0.01
GA	Objective Function (pu)	N_P	CPU time (sec)	P_c	P_m
	0.0138	5	293.4507	0.5	0.01
HDE	Objective Function (pu)	N_P	CPU time (sec)	C_R	F
	0.0002	5	76.8322	0.5	0.01

TABLE III
PARAMETER VALUES OF PSSS DESIGNED UNDER OPERATION CONDITION 1

		K_S	T_1 (sec)	T_2 (sec)	T_3 (sec)	T_4 (sec)	T_5 (sec)
DE	G2	21.1	0.97	0.13	0.85	1.02	0.50
	G4	7.14	1.80	0.22	0.79	0.02	0.50
	G7	39.5	1.80	0.01	0.86	0.78	0.50
	G9	16.1	1.78	1.78	0.66	1.88	0.50
	G10	18.6	1.81	0.17	1.66	0.44	0.50
GA	G2	45.3	1.66	0.69	1.08	0.26	0.50
	G4	18.4	0.02	0.57	0.03	1.88	0.50
	G7	48.7	1.08	0.019	1.43	1.45	0.50
	G9	49.6	1.53	0.55	1.35	0.14	0.50
	G10	49.5	1.80	0.24	1.99	0.25	0.50
HDE	G2	16.0	0.58	0.10	1.95	0.34	0.50
	G4	14.2	0.25	0.17	0.62	0.02	0.50
	G7	29.2	0.23	0.05	0.84	0.04	0.50
	G9	45.7	1.67	0.24	1.64	0.25	0.50
	G10	48.4	1.87	0.27	2.00	0.24	0.50

TABLE IV
ELECTROMECHANICAL MODES WITH PSSS

DE	GA	HDE
Eigenvalue (Damping Ratio)	Eigenvalue (Damping Ratio)	Eigenvalue (Damping Ratio)

-3.19 ± j 7.41 (0.41)	-2.08 ± j 8.57 (0.24)	-2.30 ± j 7.64 (0.29)
-1.04 ± j 3.71 (0.27)	-1.28 ± j 4.90 (0.25)	-1.46 ± j 7.69 (0.19)
-0.82 ± j 2.38 (0.32)	-1.17 ± j 8.95 (0.13)	-1.28 ± j 8.55 (0.15)
-0.73 ± j 7.52 (0.10)	-1.11 ± j 6.42 (0.17)	-1.28 ± j 4.53 (0.27)
-0.43 ± j 7.02 (0.06)	-0.63 ± j 7.35 (0.09)	-1.04 ± j 9.34 (0.11)
-0.41 ± j 8.84 (0.05)	-0.59 ± j 8.92 (0.07)	-0.82 ± j 8.95 (0.09)
-0.38 ± j 8.19 (0.05)	-0.58 ± j 6.84 (0.08)	-0.82 ± j 8.95 (0.09)
-0.33 ± j 6.54 (0.05)	-0.57 ± j 9.22 (0.06)	-0.74 ± j 7.15 (0.10)
-0.33 ± j 5.95 (0.06)	-0.41 ± j 9.18 (0.04)	-0.68 ± j 6.43 (0.11)

TABLE V

PARAMETER VALUES OF PSSS USING HDE DESIGN UNDER OPERATION CONDITIONS 1-3

	K_S	T_1 (sec)	T_2 (sec)	T_3 (sec)	T_4 (sec)	T_5 (sec)
G2	26.4	1.37	0.01	1.19	1.07	0.50
G4	2.72	1.42	0.01	1.96	0.43	0.50
G7	22.8	0.96	0.35	1.03	0.01	0.50
G9	46.6	2.00	0.27	2.00	0.30	0.50
G10	43.9	1.99	0.29	2.00	0.20	0.50

TABLE VI

ELECTROMECHANICAL MODES WITH PSSS USING HDE DESIGN UNDER OPERATION CONDITION 1 AND OPERATION CONDITION 1-3

Design condition	under operation condition 1	under operation condition 1-3
Operation condition 1 Eigenvalue (Damping Ratio)	-2.30 ± j 7.64 (0.29)	-2.20 ± j 4.16 (0.47)
	-1.46 ± j 7.69 (0.19)	-2.02 ± j 5.54 (0.34)
	-1.28 ± j 8.55 (0.15)	-2.01 ± j 8.01 (0.24)
	-1.28 ± j 4.53 (0.27)	-1.41 ± j 9.16 (0.15)
	-1.04 ± j 9.34 (0.11)	-1.25 ± j 7.79 (0.16)
	-0.82 ± j 8.95 (0.09)	-0.98 ± j 9.03 (0.11)
	-0.82 ± j 8.95 (0.09)	-0.74 ± j 8.88 (0.08)
	-0.74 ± j 7.15 (0.10)	-0.74 ± j 7.53 (0.10)
	-0.68 ± j 6.43 (0.11)	-0.72 ± j 6.50 (0.11)
Operation condition 2 Eigenvalue (Damping Ratio)	-2.32 ± j7.64 (0.30)	-2.32 ± j 5.62 (0.38)
	-1.51 ± j4.43 (0.32)	-2.14 ± j 3.93 (0.48)
	-1.43 ± j7.66 (0.18)	-2.04 ± j 8.01 (0.25)
	-1.20 ± j8.45 (0.14)	-1.40 ± j 9.14 (0.15)
	-1.03 ± j9.32 (0.11)	-1.11 ± j 7.78 (0.14)
	-0.98 ± j7.02 (0.14)	-0.95 ± j 9.02 (0.10)
	-0.84 ± j8.84 (0.09)	-0.85 ± j 7.54 (0.11)
	-0.78 ± j9.03 (0.09)	-0.77 ± j 8.86 (0.09)
	-0.55 ± j6.29 (0.09)	-0.61 ± j 6.22 (0.10)
Operation condition 3 Eigenvalue (Damping Ratio)	-2.29 ± j 7.57 (0.29)	-2.64 ± j 6.79 (0.36)
	-1.82 ± j 7.93 (0.22)	-2.05 ± j 7.97 (0.25)
	-1.23 ± j 8.54 (0.14)	-1.58 ± j 3.53 (0.41)
	-1.20 ± j 4.02 (0.29)	-1.36 ± j 9.07 (0.15)
	-0.99 ± j 9.21 (0.11)	-1.12 ± j 7.82 (0.14)
	-0.86 ± j 8.79 (0.10)	-0.87 ± j 8.79 (0.10)
	-0.78 ± j 9.15 (0.08)	-0.84 ± j 9.10 (0.09)
	-0.54 ± j 6.89 (0.08)	-0.76 ± j 6.82 (0.11)
	-0.47 ± j 5.91 (0.08)	-0.63 ± j 5.97 (0.10)

TABLE VII

PARAMETER VALUES OF PSSS USING HDE WITH DIFFERENT OBJECTIVE FUNCTIONS

Objective function		K_S	T_1 (sec)	T_2 (sec)	T_3 (sec)	T_4 (sec)	T_5 (sec)
M_1	G2	35.5	0.99	1.02	0.89	0.05	0.50
	G4	11.0	0.33	0.40	1.09	0.02	0.50
	G7	48.7	1.90	0.31	1.24	0.04	0.50
	G9	28.1	1.97	0.29	1.20	0.11	0.50
	G10	30.3	1.85	0.12	0.97	0.17	0.50
M_2	G2	25.5	1.41	1.64	1.96	0.03	0.50
	G4	5.08	0.65	0.10	0.54	0.01	0.50
	G7	14.1	0.78	0.12	1.22	0.02	0.50
	G9	50.0	2.00	0.27	1.65	0.25	0.50
	G10	37.6	2.00	0.20	1.76	0.22	0.50

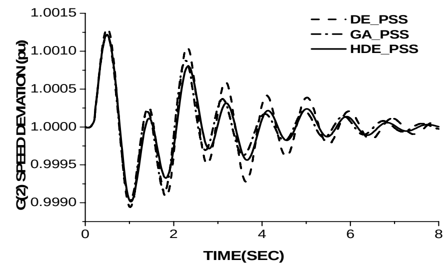

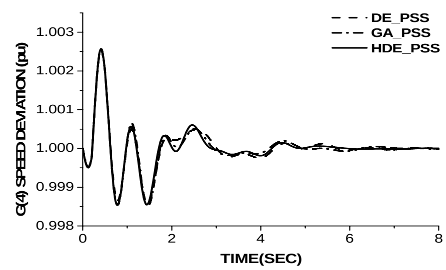

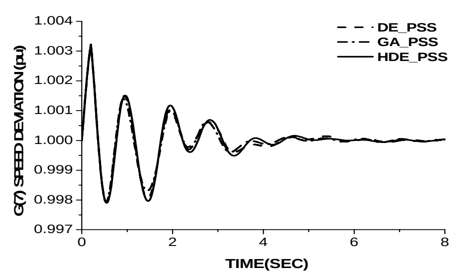

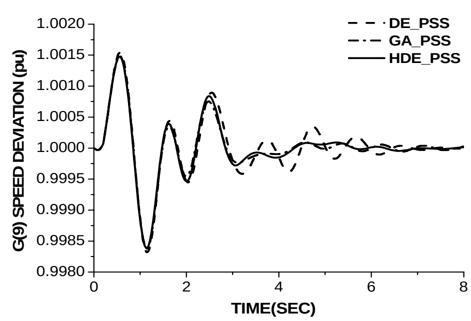

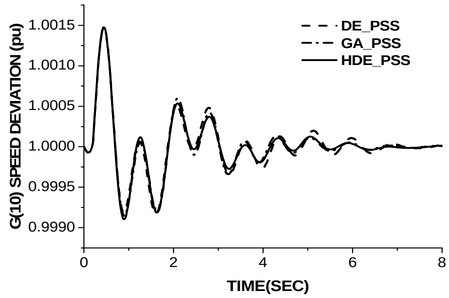

Fig. 6. Responses of Generators 2, 4, 7, 9, and 10 subjected to large disturbance

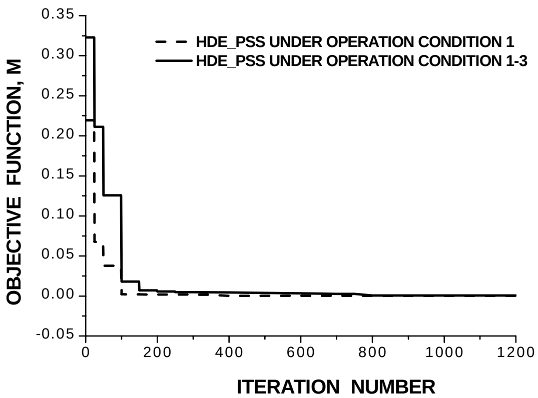

Fig. 7. Convergent characteristics of objective functions M using HDE under different operation conditions

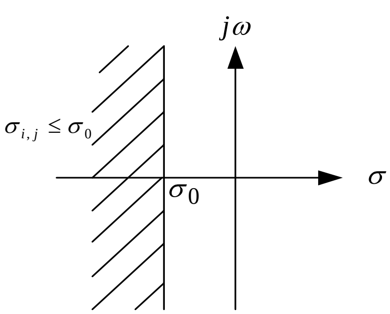

Fig. 8. A region where

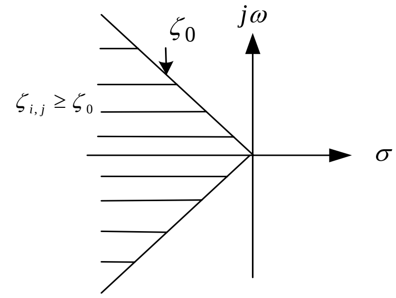

Fig. 9. A region where $\zeta_{i,j} \ge \zeta_0$

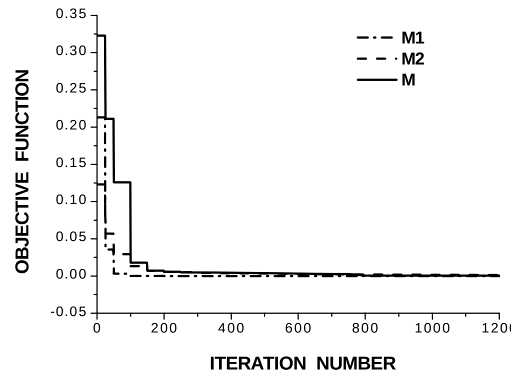

Fig. 10. Convergent characteristics of objective functions M, M1, and M2 using HDE

TABLE VIII

ELECTROMECHANICAL MODES USING HDE WITH DIFFERENT OBJECTIVE FUNCTIONS DESIGNED UNDER OPERATION CONDITION 1-2

Objective function	M_1	M_2	M
Operation condition 1 Eigenvalue (Damping Ratio)	-3.60 ± j6.82 (0.47)	-2.29 ± j8.15 (0.27)	-2.20 ± j4.16 (0.47)
	-2.42 ± j7.04 (0.33)	-1.46 ± j8.95 (0.16)	-2.02 ± j5.54 (0.34)
	-1.09 ± j3.34 (0.31)	-1.40 ± j7.96 (0.17)	-2.01 ± j8.01 (0.24)
	-0.88 ± j9.39 (0.09)	-1.23 ± j4.10 (0.29)	-1.41 ± j9.16 (0.15)
	-0.88 ± j8.24 (0.11)	-0.98 ± j8.95 (0.11)	-1.25 ± j7.79 (0.16)
	-0.74 ± j5.63 (0.13)	-0.84 ± j5.91 (0.14)	-0.98 ± j9.03 (0.11)
	-0.56 ± j7.65 (0.07)	-0.76 ± j7.66 (0.10)	-0.74 ± j8..88 (0.08)
	-0.53 ± j6.70 (0.08)	-0.79 ± j6.76 (0.12)	-0.74 ± j7.53 (0.10)
	-0.51 ± j8.85 (0.06)	-0.65 ± j8.86 (0.07)	-0.72 ± j6.50 (0.11)

Operation condition 2 Eigenvalue (Damping Ratio)	-3.76 ± j6.89 (0.48)	-2.32 ± j8.15 (0.27)	-2.32 ± j5.62 (0.38)
	-2.32 ± j6.98 (0.32)	-1.44 ± j8.92 (0.16)	-2.14 ± j3.93 (0.48)
	-0.98 ± j3.09 (0.30)	-1.35 ± j4.08 (0.31)	-2.04 ± j8.01 (0.25)
	-0.87 ± j9.37 (0.09)	-1.25 ± j7.94 (0.16)	-1.40 ± j9.14 (0.15)
	-0.85 ± j5.70 (0.15)	-1.06 ± j6.09 (0.17)	-1.11 ± j7.78 (0.14)
	-0.81 ± j8.21 (0.10)	-0.98 ± j8.94 (0.11)	-0.95 ± j9.02 (0.11)
	-0.57 ± j7.63 (0.07)	-0.79 ± j7.68 (0.10)	-0.85 ± j7.54 (0.11)
	-0.55 ± j6.34 (0.09)	-0.65 ± j8.85 (0.07)	-0.77 ± j8.86 (0.09)
	-0.51 ± j8.84 (0.06)	-0.59 ± j6.19 (0.09)	-0.61 ± j6.22 (0.10)

TABLE IX
COHERENCY MEASURES OF THE SYSTEM WITHOUT PSS

	G2	G3	G4	G5	G6	G7	G8	G9	G10
G2	1.00	0.94	0.47	0.84	0.13	0.23	0.80	0.81	0.79
G3	0.94	1.00	0.50	0.82	0.14	0.23	0.84	0.78	0.82
G4	0.47	0.50	1.00	0.35	0.38	0.41	0.62	0.48	0.66
G5	0.84	0.82	0.35	1.00	0	0.11	0.67	0.77	0.65
G6	0.13	0.14	0.38	0	1.00	0.85	0.24	0.19	0.27
G7	0.23	0.23	0.41	0.11	0.85	1.00	0.32	0.31	0.35
G8	0.80	0.84	0.62	0.67	0.24	0.32	1.00	0.71	0.94
G9	0.81	0.78	0.48	0.77	0.19	0.31	0.71	1.00	0.72
G10	0.79	0.82	0.66	0.65	0.27	0.35	0.94	0.72	1.00

TABLE X
COHERENCY MEASURES OF THE SYSTEM WITH PSSS

	G2	G3	G4	G5	G6	G7	G8	G0	G10
G2	1.00	0.87	0.62	0.78	0.20	0.33	0.82	0.84	0.83
G3	0.87	1.00	0.60	0.77	0.11	0.27	0.84	0.78	0.81
G4	0.62	0.60	1.00	0.45	0.30	0.45	0.70	0.59	0.75
G5	0.78	0.77	0.45	1.00	0	0.13	0.65	0.78	0.64
G6	0.20	0.11	0.30	0	1.00	0.82	0.22	0.18	0.27
G7	0.33	0.27	0.45	0.13	0.82	1.00	0.37	0.32	0.41
G8	0.82	0.84	0.70	0.65	0.22	0.37	1.00	0.70	0.92
G9	0.84	0.78	0.59	0.78	0.18	0.32	0.70	1.00	0.72
G10	0.83	0.81	0.75	0.64	0.27	0.41	0.92	0.72	1.00

V. CONCLUSION

A comprehensive decentralized pole assignment method based on HDE has been successfully used in the design of lead-lag phase compensation power system stabilizers. A multi-machine system is used as an example to demonstrate the developed method and reveal the convergent procedures. The participation factors associated with the electromechanical modes are used to select the sites of power system stabilizers. The computation time and the convergent characteristics of the objective function are better, compared with that from GA and DE. The chosen region to assign the electromechanical modes could be relatively important in the design. From the simulation results, the HDE gives a good method in tuning power system stabilizers to improve system dynamic stability. The coherency analysis results reveal that the levels of similarity between any pair of generators have been kept.

ACKNOWLEDGMENT

The paper is partly supported by the Taipei College of Maritime Technology and the National Science Council of Taiwan, project number, NSC 95-2221-E-011-187.

REFERENCES

[1] Y. Hong and W. Wu, "A new approach using optimization for tuning parameters of power system stabilizers," *IEEE Transactions on Energy Conversion*, Vol. 14, No. 3, pp. 780-786, 1999.

[2] M. Abido, "Robust design of multimachine power system stabilizers using simulated annealing," *IEEE Transactions on Energy Conversion*, Vol. 15, No. 3, pp. 297–304, 2000.

[3] C. Tse, K. Wang, C. Chung, and K. Tsang, "Parameter optimization of robust power system stabilisers by probabilistic approach," *IEE Proceedings Generation, Transmission and Distribution*, Vol. 147, No. 2, pp. 69-75, 2000.

[4] M. Abido and Y. Abdel-Magid, "Robust design of multimachine power system stabilisers using Tabu search algorithm," *IEE Proceedings Generation, Transmission and Distribution*, Vol. 147, No. 6, pp. 387-394, 2000.

[5] M. Abido, "Optimal design of power system stabilizers using particle swarm optimization, *IEEE Transactions on Energy Conversion*," Vol. 17, No. 3, pp. 406–413, 2002.

[6] Y. Abdel-Magid and M. Abido, "Optimal multiobjective design of robust power system stabilizers using genetic algorithms," *IEEE Transaction on Power Systems*, Vol. 18, No. 3, pp. 1125-1132, 2003.

[7] Y. Li, F. Wang, and K. Hwang, "A hybrid method of evolutionary algorithms for mixed-integer nonlinear optimization problems," *Proceedings of the Congress on Evolutionary Computation*, Vol. 3, No. 1, pp2159-2166, 1999.

[8] Y. Lin, K. Hwang, and F. Wang, "Hybrid differential evolution with multiplier updating method for nonlinear constrained optimization problems," *Proceedings of the Congress on Evolutionary Computation*, Vol. 1, No. 1, pp. 872-877, 2002.

[9] J. Chiou and F. Wang, "A hybrid method of differential evolution with application to optimal control problems of a bioprocess system," *Proceedings of the Congress on Evolutionary Computation*, Vol. 1, No. 1, pp. 627-632, 1998.

[10] F. Wang and H. Jang, "Parameter estimation of a bioreaction model by hybrid differential evolution," *Proceedings of the Congress on Evolutionary Computation*, Vol. 1, No. 1, pp. 410-417, 2000.

[11] U. Lin, K. Hwang, and F. Wang, "Plant scheduling and planning using mixed-integer hybrid differential evolution with multiplier updating," *Proceedings of the Congress on Evolutionary Computation*, Vol. 1, No. 1, pp. 593-600, 2000.

[12] C. Su and C. Lee, "Network reconfiguration of distribution systems using improved mixed-integer hybrid differential evolution," *IEEE Transactions on Power Delivery*, Vol. 18, No. 3, pp. 1022-1027, 2003.

[13] C. Su and C. Lee, "Modified differential evolution method for capacitor placement of distribution systems," *Asia Pacific IEEE/PES Transmission*

and Distribution Conference and Exhibition, Vol. 1, No. 1, pp. 208-213, 2002.

[14] T. L. Huang, K. T. Lee, C. H. Chang, and T. Y. Hwang, "Sliding Mode Power System Stabilizer using Artificial Immune Algorithm," *WSEAS Transactions on Power Systems*, Vol. 1, No. 10, pp. 1707-1712, 2006.

[15] J. R. Pacheco and J. Salinas, "Modelling And Control Techniques For Tuning Stabilizers In Power Systems," *Proceedings of the 6th WSEAS International Conference on Circuits, Systems, Electronics, Control & Signal Processing (CSECS'07)*, Dec. 29-31, pp.239-244, 2007.

[16] K. Turkoglu and E. M. Jafarov, "Application of H inf. Loop Shaping Robust Control System Design on Longitudinal Dynamics of Hezarfen UAV with Classical PI(D) and Pole Placement Methods: A Comparison Analysis," *WSEAS Transactions on Power Systems*, Vol. 6, No. 1, pp. 206-213, 2007.

[17] K. Zakova, "Constrained Pole Assignment Controller for Delayed Double Integrator System," *Proceedings of the 6th WSEAS International Conference on System Science and Simulation in Engineering (ICOSSSE)*, Nov. 21-23, pp.12-17, 2007.

[18] M. Pai, *Energy function analysis for power system stability*, Kluwer, Norwell, Massachusetts, 1989.

Yung-Sung Chuang was born in Taiwan, 1962. He received the B. Sc., and M. Sc., and Ph. D. degree in electrical engineering all from the National Taiwan University of Science and Technology in 1989, 1991, and 2006, respectively. Now he is an associate professor in the Department of Electrical Engineering, Ming Hsin University of Science and Technology. His research interests include power system control and design, electric power quality, and system identification.

Shu-Chen Wang was born in Taiwan, 1969. She received the B. Sc., M. Sc., and Ph.D. degree from the Department of Electrical Engineering, National Taiwan Ocean University in 1992, 1994, and 2007, respectively. Currently she is an associate professor in the Department of Computer and Communication Engineering, Taipei College of Maritime Technology. Her current research interests include fuzzy theory and power system dynamics.

Chi-Jui Wu was born in Taiwan, 1961. He received the B. Sc., M. Sc., and Ph.D. degree in electrical engineering all from the National Taiwan University in 1983, 1985, and 1988, respectively. In 1988, he joined the Department of Electrical Engineering, National Taiwan University of Science and Technology. Now he is a full professor in the Department. He is active in practical power system problems. His current research interests lie in power system stability, power electromagnetic interference, and electric power quality.